Original Article

Three-dimensional alteration of constricted alveolar ridge affected by root thrusting with and without open-flap decortication

Donghyun Hwang[a]; Won-June Lee[b]; Kyung-A Kim[c]; Seung-Hak Baek[d]; Young-Guk Park[e]; Su-Jung Kim[f]

ABSTRACT

Objective: To investigate the morphometric and histological alterations of the constricted alveolar ridge when affected by root thrusting with and without open-flap decortication.

Materials and Methods: Eight beagles were divided into three groups: C, control without root thrusting; R, root thrusting only; RD, root thrusting with alveolar decortication. The ridge constriction model was prepared in 16 mandibular quadrants after extraction of the third premolars. Reciprocal root thrusting of the second and fourth premolars was performed toward the constricted ridge for 10 weeks, having a moment of 900 g-mm. Open-flap decortication was conducted on the constricted bone surface in group RD. Micro-CT-based histomorphometric analysis and trichrome-staining-based tissue fractional analysis were performed to evaluate morphometric and microstructural changes on the ridge.

Results: Group R revealed a higher percentage of bone volume ($P < .001$), lower bone mineral density ($P < .01$), and higher trabecular number ($P < .001$) than did group C, which was supported by a higher bone fraction woven to lamellar bone ($P < .05$) resulting from histologic fractional analysis. However, group RD showed no significant difference from group C.

Conclusions: Root thrusting toward the constricted ridge induced hypertrophic bone modeling with a high trabecular fraction on the ridge. However, combined open-flap decortication with root thrusting did not improve the volume or quality of the constricted ridge. (*Angle Orthod.* 2017;87:725–732.)

KEY WORDS: Constricted alveolar ridge; Root thrusting; Open-flap decortication; Bone modeling; Histological tissue fraction

INTRODUCTION

Orthodontic tooth movement (OTM) through the atrophic alveolar ridge is still challenging and unpredictable in current practice. Constriction of the alveolar ridge occurs mostly and more rapidly in a horizontal direction, narrowing the ridge width by up to 50% of its original dimension in the first 12 months after tooth extraction.[1] As ridge atrophy progresses, bone mineral density in both cortical and trabecular bones may change,[2] relating to a decrease in vascularity to evoke cellular recruitment for bone remodeling or repair.[3,4] Although scientific controversy persists on whether it is possible to move the teeth efficiently through the constricted alveolar ridge to close space, clinical consensus exists that the periodontal risks of bony dehiscence and further attachment loss will be increased around the moved teeth.[5,6]

An interesting orthodontic trial designed to overcome this limitation found coronal increments of bone height on the preexisting atrophic ridge by well-controlled

[a] Postgraduate Student, Kyung Hee University Graduate School, Seoul, Korea.
[b] Graduate Student, Kyung Hee University Graduate School, Seoul, Korea.
[c] Assistant Professor, Department of Orthodontics, Kyung Hee University School of Dentistry, Seoul, Korea.
[d] Professor, Department of Orthodontics, School of Dentistry, Dental Research Institute, Seoul National University, Seoul, Korea.
[e] Professor, Department of Orthodontics, Kyung Hee University School of Dentistry, Seoul, Korea.
[f] Associate Professor, Department of Orthodontics, Kyung Hee University School of Dentistry, Seoul, Korea.
Corresponding author: Dr Su-Jung Kim, Department of Orthodontics, Kyung Hee University School of Dentistry, 1 Hoegi-Dong, Dongdaemoon-Ku, Seoul 130-701, Korea
(e-mail: ksj113@khu.ac.kr)

Accepted: May 2017. Submitted: March 2017.
Published Online: July 14 2017

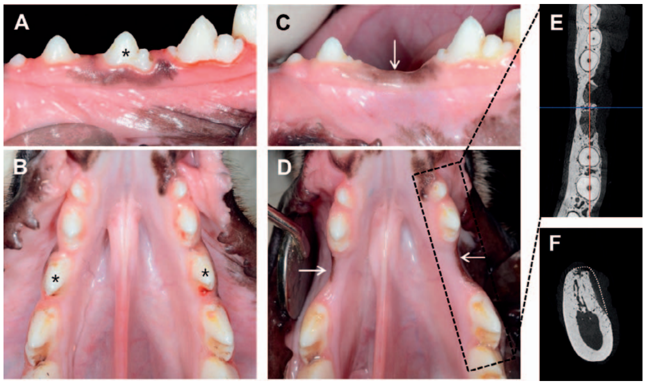

Figure 1. Prepared beagle model with constricted alveolar ridge in the mandible. A and B, sound periodontium before extraction of third premolar (*). C and D, vertically and horizontally constricted alveolar ridge (indicated by white arrows) at 4 weeks after extraction. E and F, micro-CT sectional images at 4 weeks after extraction.

bodily tooth movement toward the ridge.[7] Instead of marginal bone resorption by compression on the side toward which a tooth crown was tipped, root dominant movement induced coronal bone apposition even on the side ahead of the moving root, which was interpreted as being related to the piezoelectric effect of bone-bending theory.[8,9] It was postulated that bending of alveolar bone by root-targeted force application gave rise to electrical potentials to enhance external bone apposition on the ridge in addition to internal biological bone remodeling. However, there has been no experimental evidence on the three-dimensional quantitative alteration of the atrophic bony ridge interposed between the moved roots.

As an adjunctive surgical procedure to improve matrix volume on the poor periodontium for subsequent OTM, ridge augmentation with bone grafting or guided bone regeneration has been widely applied.[9–14] However, these regenerative procedures have limited success for graft survival in cases of severe tissue constriction with poor vascularity in the remaining alveolar ridge.[13] Corticotomy, or decortication, which involves removing some part of the cortical bone instead of building up matrix volume, was introduced to decrease tissue resistance in the atrophic bone based on the regional acceleratory phenomenon (RAP), thereby increasing bone turnover and decreasing bone density.[14] So far, faster tooth movement has been perceived as the major benefit of these decortication procedures.[15–17] Any periodontal response on the previously constricted alveolar ridge induced by surgically-assisted tooth movement has not been a central focus.

The present study aimed to investigate and compare morphometric and histological alterations of the constricted alveolar ridge affected by root thrusting with and without open-flap decortication, with regard to volumetric bone modeling, structural bone remodeling, and histologic tissue fraction.

MATERIALS AND METHODS

This research was approved by the Institutional Animal Ethical Committee (15-025). Eight male beagles (aged 18–24 months; weight, 10–12 kg) were housed in separate cages following the guidelines of Kyung Hee University Medical Center-Institutional Animal Care and Use Committee. The animal model with a constricted alveolar ridge was prepared in 16 mandibular quadrants 4 weeks after extraction of both third premolars. Natural socket healing occurred without periodontal inflammation, producing ridge constriction in both the vertical and buccolingual dimensions (Figure 1). The animals were randomly divided into three groups: C, control without treatment; R, root thrusting only; RD, root thrusting with decortication (Figure 2).

Reciprocal traction of the second and the fourth premolars by root dominant movement (root thrusting) rather than by crown tipping was performed towards the constricted ridge for 10 weeks (Figure 2). Orthodontic brackets (Tomy Co, Tokyo, Japan) were bonded on two premolars, and a sectional spring with a double helix fabricated from 0.017×0.025-inch stainless steel wire (Tru-Chrome SS, Rocky Mountain Orthodontics, Denver, Colo) was inserted between the teeth. Effective tipback bends of 15° were applied on both spring ends to exert a root thrusting couple (700 g-mm $= 200$ g $\times$ 3.5 mm). A passive tie was added between the helix and its adjacent bracket to concentrate the moment exerted on the root apex, preventing crown tipping away from the constricted ridge. The appliance was checked and readjusted every 2 weeks throughout the experimental period.

Decortication was conducted immediately before initiating tooth movement. After mucoperiosteal flap reflection, cortical punches were created at six points on the buccal surface of the ridge using a No. 2 surgical round bur. The depth and width of the punches were confined to 1.5 – 2 mm using a bur diameter of 1.5 mm to insult the cancellous bone through the cortical layer. For postoperative care, analgesics (Ketopro; Uni Biotech Co, Chungnam, Korea) and antibiotics (Gentamycin; Komipharm International Co, Shiheung, Korea) were administered intramuscularly BID for 3 days, and a surgical dressing with 0.12% chlorhexidine gluconate rinse (Hexamedine Solution; Bukwang Pharm Co, Seoul, Korea) was applied daily. All animals were euthanized by direct injection of Zoletil 50 (Virbac Lab, Carros, France; 50 mL/kg) into the heart 10 weeks after OTM.

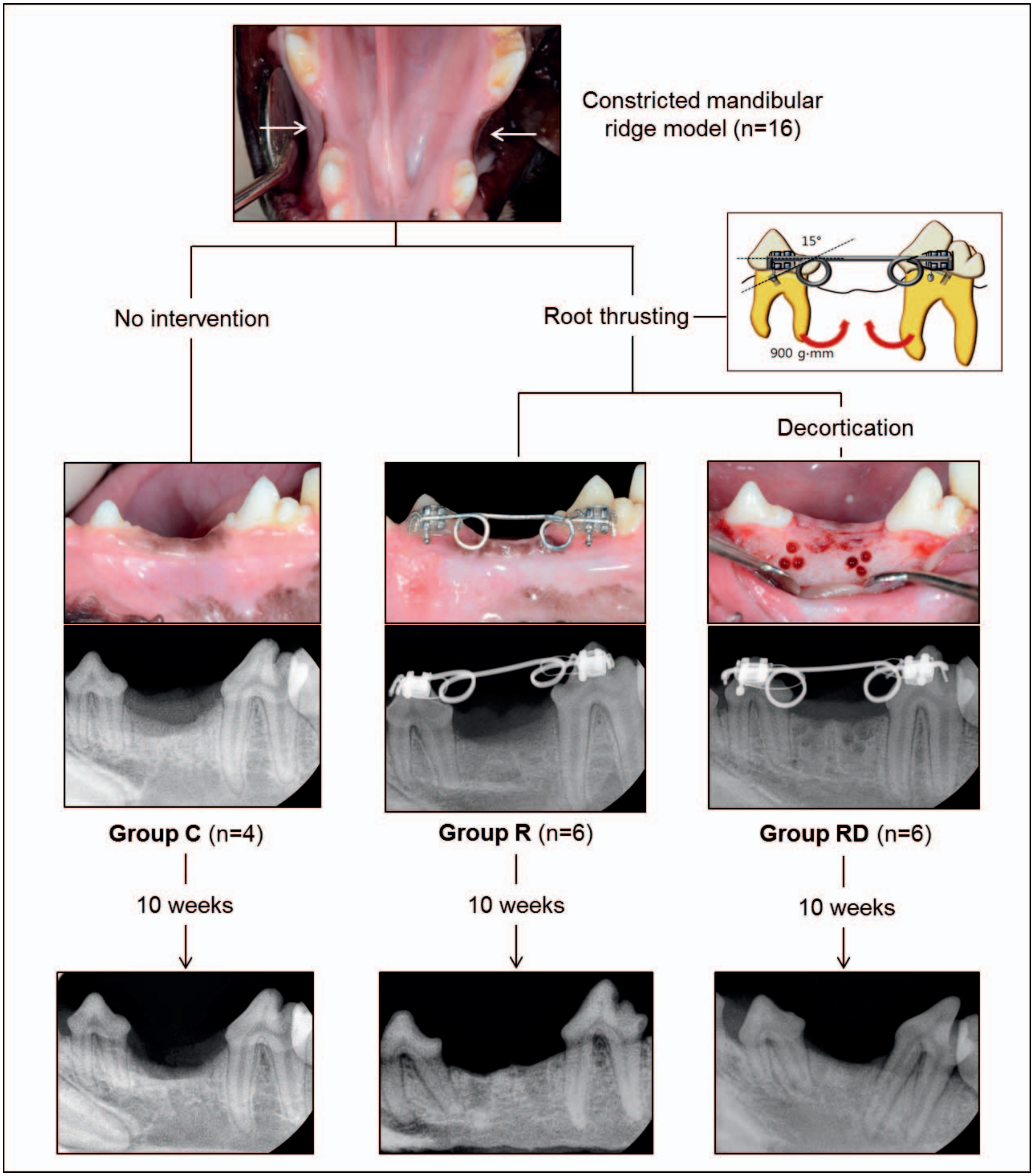

Figure 2. Diagram of experimental design. Sixteen mandibular quadrants were divided into three groups: C, control (n = 4); R, root thrusting only (n = 6); RD, root thrusting with decortication (n = 6).

Histomorphometric Analysis of Micro-CT Images

Tissue blocks including the ridge and two moved teeth were harvested and fixed by 10% formalin for 48 hours. Microcomputed tomography (micro-CT) images were obtained not only to describe the morphologic changes of the constricted ridge relating to the type of OTM, but also to analyze internal bony structures

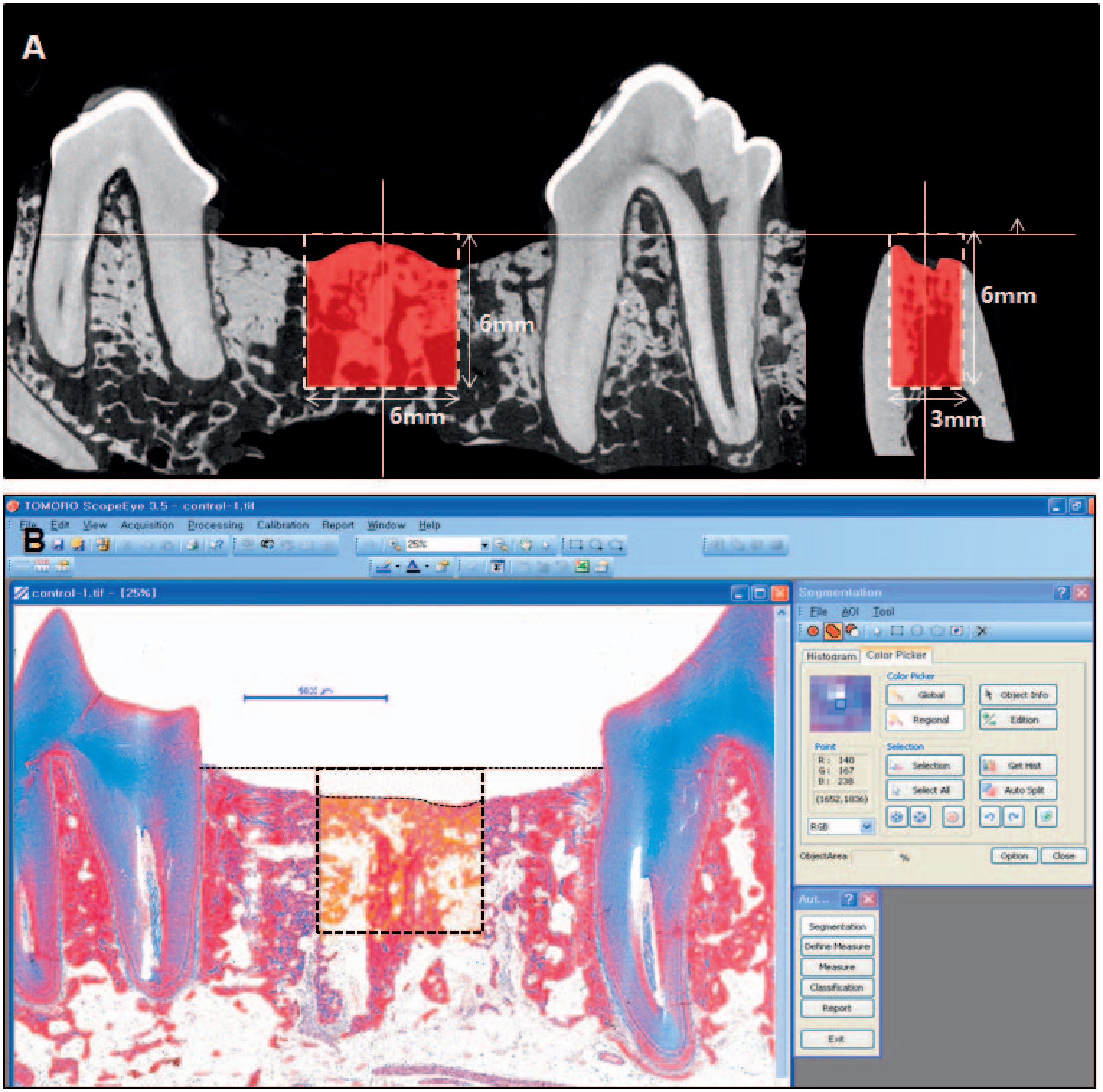

Figure 3. Procedure of designating a volume of interest on the micro-CT image for histomorphometric analysis (A) and a region of interest on the histologic section for tissue fractional analysis (B).

quantitatively. Images were taken using SkyScan 1173 (Bruker-microCT, Kontich, Belgium) with settings of 90 kVp source voltage, 88 mA of current, and 18.11μm of image pixel size. To establish a volume of interest, a $6.0 \times 6.0 \times 3.0\text{-mm}^3$ cube was first designated encompassing the central portion of the ridge in the middle between the two teeth (Figure 3A). The upper reference line of the cube constituted a plane connecting the marginal bone levels between the distal side of the second premolar and the mesial side of the fourth premolar facing the ridge of interest. Percentage bone volume (BV/CV, %) was calculated as the fraction of the total bone volume (BV) within the designated cubic volume (CV). The following five parameters were measured within the defined total bone volume, excluding the empty space in the cube: bone mineral density (g/cm^3), bone surface ratio (BS/BV, %), trabecular thickness (Tb.Th. mm), trabecular number (Tb.N. mm^{-1}), and trabecular separation (Tb.Sp. mm). Six parameters were measured from

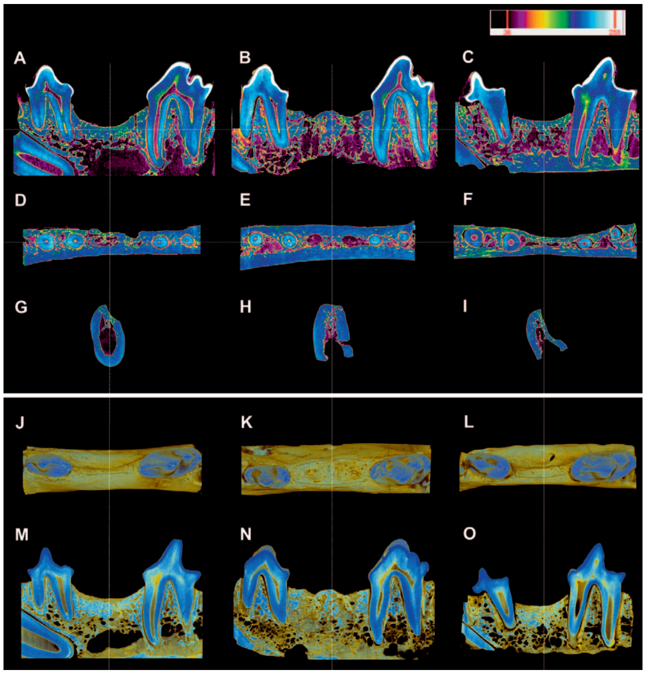

Figure 4. Micro-CT sectional and volume images. Color-mapped sectional images (A-I) show the highest vertical bone level with higher fraction of immature bone in group R (B, E, H) than in group RD (C, F, I) and group C (A, D, G), supported by reconstructed volume images (J-O).

three reconstructed images by one technician and automatically transmitted to data sets as mean values (version 1.12.0.0, CT Analyser; Bruker-microCT, Kontich, Belgium). Three-dimensional volume images were reconstructed using CTVox software (Bruker-microCT) to see all the volumetric changes of the ridge and intrabony trabecular pattern.

Histological Tissue Fractional Analysis

Fixed tissue blocks were decalcified, dehydrated, embedded in paraffin, and longitudinally sectioned in a mesiodistal direction in thicknesses of 5 μm. Masson's trichrome staining was used to discriminate immature new bone tissue from mature lamellar bone. Microphotographs were taken at 1.5$\times$ magnification under light microscopy, in which the region of interest was defined as a preset box containing the central portion of the ridge in the middle with the upper reference line connecting the marginal bone levels of two adjacent teeth (Figure 3B). Using a Tomoro Scope Eye 3.5.197 image analyzer (Samkyung Co, Seoul, Korea), which autosplits and merge planes based on automatic image segmentation by a color selection system, the proportion (%) of total mineralized bone, woven bone, lamellar bone, and bone marrow space were measured, and the ratio of woven bone to lamellar bone within the mineralized tissue was calculated. Measurements were repeated twice by one histologist.

Statistical Analysis

SPSS software 22.0 (IBM SPSS, Armonk, NY) was used with a significance level of .05. One-way ANOVA with Scheffe's post hoc analysis was performed to compare six microstructural parameters measured from three reconstructed images per sample ($n = 18$/tested group). The Kruskal-Wallis test was used for intergroup comparison of tissue component fractions from one histologic section per sample ($n = 6$/tested group). Intraobserver reliability for repeated measurements was confirmed by the Kappa coefficient of concordance as 0.823 in micro-CT and 0.701 in histologic analysis.

RESULTS

Color-mapped micro-CT sectional images were compared in three planes (Figure 4A-I). We found via mesiodistal sectional imaging that group R revealed a convex ridge contour with coronal bone increment composed of a higher ratio of less dense bone (Figure 4B), whereas Group RD showed a concave ridge contour covered with an extremely dense bony bridge (Figure 4C) similar to that of group C (Figure 4A). Cross-sectional images taken from the level of the midpoint of the mesial root of the fourth premolar indicated that group R showed the widest buccolingual thickness of the ridge (Figure 4E), while group RD revealed a narrower ridge thickness (Figure 4F) than did group C (Figure 4D), especially on the buccal surface, which was verified from buccolingual sectional images (Figure 4G-I). Three-dimensionally reconstructed volume images confirmed the intergroup differences of the morphological outline of the ridge (Figure 4J-O). The widest buccolingual bone thickness at the crestal level was observed in group R, with a convex contour on the buccal surface (Figure 4K), whereas a thin bony crest with a concave buccal plate was found in group RD (Figure 4L). The trabecular pattern of the half-sectional volume images was different among the groups (Figure 4M-O), quantitatively compared by histomorphometric analysis (Table 1). Group R exhibited a significantly higher percentage bone volume ($P < .001$), lower bone mineral density ($P < .01$), higher trabecular number ($P < .001$), and lower trabecular thickness ($P < .001$) than did group RD. Group RD was not significantly different from group C, except for bone surface ratio ($P < .05$) and trabecular thickness ($P < .001$). Trabecular separation was not significantly different among groups.

Histological findings indicated completely healed sockets covered with intact crestal bridges in all groups

Table1. Intergroup Comparison of Six Microstructural Parameters Based on Histomorphometric Analysis of Three-Dimensional Micro-CT Volume of Interest[a]

Description (Mean ± SD)	Abbreviation (unit)	Group C (n = 12)	Group R (n = 18)	Group RD (n = 18)	*P* value	Scheffe's Post Hoc Comparison
Bone mineral density	BMD (g/cm^3)	0.60 ± 0.06	0.41 ± 0.86	0.54 ± 0.15	.002**	R < C, RD
Percent bone volume	BV/TV (%)	31.31 ± 3.47	50.63 ± 7.29	34.85 ± 3.58	.000***	R > C, RD
Bone surface ratio	BS/BV (%)	3.56 ± 0.31	4.69 ± 0.35	4.59 ± 0.21	.012*	R, RD > C
Trabecular thickness	Tb.Th (mm)	0.87 ± 0.12	0.69 ± 0.07	0.76 ± 0.11	.000***	C > R, RD
Trabecular number	Tb.N (mm^{-1})	0.35 ± 0.09	0.58 ± 0.09	1.41 ± 0.07	.000***	RD > C, R
Trabecular separation	Tb.Sp (mm)	1.93 ± 0.10	2.05 ± 0.22	1.94 ± 0.15	.208	NS[b]

[a] Tested by ANOVA and Scheffe's post hoc comparison.
[b] NS indicates no significance; *, $P < .05$; **, $P < .01$; ***, $P < .001$.

(Figure 5). Group R showed coronal bone apposition at the center of the ridge consisting of composite bone (Figure 5B), whereas group RD had highly matured lamellar bone with a smaller bone marrow cavity (Figure 5C). As a result of tissue fractional analysis (Table 2), total mineralized bone volume within the designated box was the greatest in group R ($P < .05$). Woven bone fraction within the total mineralized bone was highest in group R and lowest in group RD ($P < .05$): 48.5% in group R, 32.3% in group C, and 24.2% in group RD.

DISCUSSION

The present study showed that, in beagles, reciprocal root thrusting toward the constricted ridge increased bone volume of the ridge in three dimensions. Root thrusting resulted in a higher fraction of woven bone and yielded a favorable matrix for further root movement. Additionally, bone appositional remodeling was observed in the marginal bone ahead of the root movement. On the other hand, combined open-flap decortication with root thrusting did not bring about volumetric or microstructural improvement of the constricted ridge.

Biological mechanisms caused by root thrusting resulted in tissue changes of the atrophic ridge. Presumably, cancellous activation triggered by root thrusting exerted not only stress-strain-dependent, multicellular, cancellous activation but also bone bending with enough of a moment to evoke active osteogenic piezoelectricity on the edentulous ridge surface.[5,7] According to a recently proposed mechanobiological principle derived from the mechanostat theory,[18,19] woven bone formed on the alveolar ridge, thereby increasing bone mass ahead of the tooth movement while the alveolar wall facing the moving tooth was resorbed. Frost[18] described the mechanostat theory of bone remodeling and modeling in terms of microstrain values, indicating that woven bone forms as a dose-dependent response to high-level tissue strain exceeding the range of the adaptive window. The root thrusting moment in the current model might have evoked tissue strain in the edentulous ridge exceeding the adaptive window level and below the pathologic overloading level of microstrain. Therefore, the result was hypertrophic woven bone production.[19] Consequently, bone density in the ridge was reduced in group R by a balance between bone formation and resorption that evoked multiple biological signaling pathways.[20–23] Simultaneously, marginal bone apposition could have been induced on the alveolar wall ahead of the thrusting roots by the load exerted by the stretched PDL that caused subsequent alveolar wall bending.[7,19] Alveolar bone compressed by the root apex was loaded less than the cervical bone experiencing tension. Tension was more dominant than

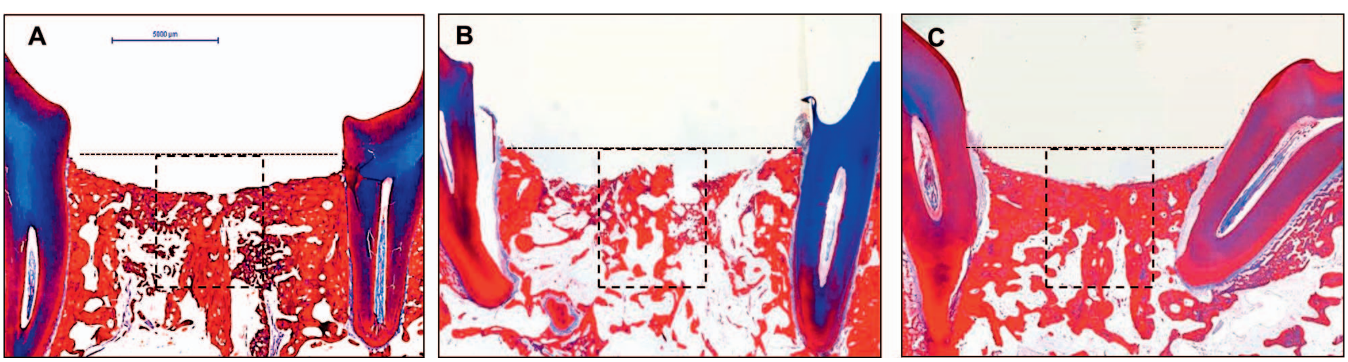

Figure 5. Microphotographs of histologic sections stained with Masson's trichrome: A, group C; B, group R; C, group RD. Note coronal bone apposition on the ridge composed of composite bone in group R. Dotted box indicates a region of interest for tissue component analysis.

Table 2. Proportion of Tissue Components Within the Designated Box Measured by TomoroScopeEye 3.5.197[a]

Description (Mean ± SD)	Group C (n = 4)	Group R (n = 6)	Group RD (n = 6)	*P* Value
Mineralized bone (MB, %)	47.3 ± 5.0	66.2 ± 6.2	52.1 ± 8.9	.024*
Bone marrow (%)	18.2 ± 3.2	15.3 ± 4.0	10.1 ± 2.1	.104
Woven bone (WB, %)	15.3 ± 3.3	32.1 ± 7.2	12.6 ± 4.5	.037*
Lamellar bone (LB, %)	32.1 ± 5.3	34.1 ± 7.3	39.5 ± 7.2	1.022
WB/MB ratio (%)	32.3	48.5	24.2	–
WB/LB ratio (%)	47.6	94.1	31.9	–

[a] Indicates analyzed by Kruskal-Wallis test; *, $P < .05$

compression when the PDL was considered as a viscoelastic nonlinear material by the mechanobiological principle.[19]

On the other hand, decortication-assisted root thrusting into the atrophic ridge did not alter the volume of the ridge (Figures 4O and 5C). Decortication, which was introduced as an efficient aid to accelerate tooth movement, has also been applied to encourage space closure through the constricted ridge.[15,24,25] Some reports suggest that corticotomy enabled OTM even through a knife-shaped alveolar ridge.[26] However, alveolar support around the moved teeth was not discussed. Poor periodontal regeneration and little bone formation are frequently observed around or ahead of moving teeth when surgically-assisted accelerated tooth movement is attempted through deficient bone. The present study results suggest that group RD might have experienced an exceptionally high immediate tissue strain of pathological levels that evoked a negative balance during the bone repair process. That strain subsequently dissipated quickly during the 4-week postdecortication due to the highly osteopenic state of the bone caused by surgically induced RAP. This is in contrast to the findings in group R, which showed that turnover of alveolar bone ahead of thrusting roots remained high after 10 weeks and kept inducing woven bone formation. Additionally, the impact of flap reflection on the response of the underlying bone needs to be considered since a full-thickness flap itself can result in the reduction of alveolar bone volume and density.[27] Nonetheless, bone mineral density was recovered 10 weeks post-surgery in group RD, exceeding the level in group R.

The animal model and design of this study included some limitations: small sample size, a partially constricted ridge instead of a completely atrophic ridge, and the difference in biological metabolic cycles between dogs and humans.[28] Still, the clinical significance of the current study is that open-flap decortication is not recommended if the ultimate goal of surgical intervention is efficient OTM through improved alveolar bone support on a constricted ridge.

CONCLUSIONS

- Root thrusting toward the constricted ridge induced hypertrophic bone modeling with high trabecular fraction in the ridge. However, combined open-flap decortication with root thrusting did not improve the volume or quality of the constricted ridge.
- Further study is required to verify the tissue responses of the atrophic alveolar ridge to different types of tooth movement in conjunction with different modalities of surgical intervention.

ACKNOWLEDGMENT

This study was supported by a National Research Foundation (NRF) grant funded by the Korean government (2014R1A1A3052072).

REFERENCES

1. Nevins M, Camelo M, De Paoli S, Friedland B, Schenk RK, Parma-Benfenati, et al. A study of the fate of the buccal wall of extraction sockets of teeth with prominent roots. *Int J Periodontics Restorative Dent*. 2006;26:19–29.
2. Klemetti E. A review of residual ridge resorption and bone density. *J Prosthet Dent*. 1996;75:512–514.
3. Eiseman B, Johnson LR, Joseph RC. Ultrasound measurement of mandibular arterial blood supply: techniques for defining ischemia in the pathogenesis of alveolar ridge atrophy and tooth loss in the elderly? *J Oral Maxillofac Surg*. 2005;63:28–35.
4. Usumi-Fujita R, Hosomichi J, Ono N, et al. Occlusal hypofunction causes periodontal atrophy and VEGF/VEGFR inhibition in tooth movement. *Angle Orthod*. 2013;83:48–56.
5. Melsen B. Tissue reaction to orthodontic tooth movement—a new paradigm. *Eur J Orthod*. 2001;23:671–681.
6. Uribe F, Janakiraman N, Fattal AN, Schincaglia GP, Nanda R. Corticotomy-assisted molar protraction with the aid of temporary anchorage device. *Angle Orthod*. 2013;83:1083–1092.
7. Lindskog-Stokland B, Wennström JL, Nyman S, Thilander B. Orthodontic tooth movement into edentulous areas with reduced bone height. An experimental study in the dog. *Eur J Orthod*. 1993;15:89–96.
8. Roberts WE, Helm FR, Marshall KJ, Gongloff RK. Rigid endosseous implants for orthodontic and orthopedic anchorage. *Angle Orthod*. 1989;59:247–256.
9. Zengo AN, Pawluk RJ, Bassett CA. Stress-induced bioelectric potentials in the dentoalveolar complex. *Am J Orthod*. 1973;64:17–27.
10. Toygar HU, Kircelli BH. Regeneration of multiple adjacent bone dehiscences with guided tissue regeneration after

orthodontic proclination: a corrective treatment approach. *Int J Periodontics Restorative Dent*. 2010;30:345–353.
11. Araújo MG, Carmagnola D, Berglundh T, Thilander B, Lindhe J. Orthodontic movement in bone defects augmented with Bio-Oss. An experimental study in dogs. *J Clin Periodontol*. 2001;28:73–80.
12. Kawamoto T, Motohashi N, Kitamura A, Baba Y, Suzuki S, Kuroda T. Experimental tooth movement into bone induced by recombinant human bone morphogenetic protein—2. *Cleft Palate Craniofac J*. 2003;40:538–543.
13. Hashemi HM, Javidi B. Comparison between interpositional bone grafting and osteogenic alveolar distraction in alveolar bone reconstruction. *J Oral Maxillofac Surg*. 2010;68:1853–1858.
14. Wilcko MT, Wilcko WM, Pulver JJ, Bissada NF, Bouquot JE. Accelerated osteogenic orthodontics technique: a 1-stage surgically facilitated rapid orthodontic technique with alveolar augmentation. *J Oral Maxillofac Surg*. 2009;67:2149–2159.
15. Kook YA, Lee W, Kim SH, Chung KR. Corticotomy-assisted space closure in adult patients with missing lower molars. *J Clin Orthod*. 2013;47:85–95.
16. Liem AML, Hoogeveen EJ, Jansma J, Ren Y. Surgically facilitated experimental movement of teeth: systematic review. *Brit J Oral Maxillofac Surg*. 2015;53:491–506.
17. Patterson BM, Dalci O, Darendeliler MA, Papadopoulou AK. Corticotomies and orthodontic tooth movement: a systematic review. *J Oral Maxillofac Surg*. 2016;74:453–473.
18. Frost HM. Bone's mechanostat: a 2003 update. *Anat Rec*. Part A. 2003;275:1081–1101.
19. Cattaneo PM, Dalstra M, Melsen B. The finite element method: a tool to study orthodontic tooth movement. *Dent Res*. 2005;84:428–433.
20. Baumrind S. A reconsideration of the property of the pressure tension hypothesis. *Am J Orthod*. 1969;55:12–22.
21. Epker BN, Frost HM. Correlation of bone resorption and formation with the physical behavior of loaded bone. *J Dent Res*. 1965;44:33–41.
22. Zengo AN, Bassett CA, Pawluk RJ, Prountzos G. In vivo bioelectric potentials in the dentoalveolar complex. *Am J Orthod*. 1974;66:130–139.
23. Uthgenannt BA, Kramer MH, Hwu JA, Wopenka B, Silva MJ. Skeletal self-repair: stress fracture healing by rapid formation and densification of woven bone. *J Bone Miner Res*. 2007;22:1548–1556.
24. Kim SJ, Park YG, Kang SG. Effects of corticision on paradental remodeling in orthodontic tooth movement. *Angle Orthod*. 2009;79:284–291.
25. Kim YS, Kim SJ, Yoon HJ, Lee PJ, Moon W, Park YG. Effect of piezopuncture on tooth movement and bone remodeling in dogs. *Am J Orthod Dentofacial Orthop*. 2013;144:23–31
26. Ozer M, Akdeniz BS, Sumer M. Alveolar ridge expansion-assisted orthodontic space closure in the mandibular posterior region. *Korean J Orthod*. 2013;43:302–310.
27. Yaffe A, Fine N, Binderman I. Regional accelerated phenomenon in the mandible following mucoperiosteal flap surgery. *J Periodont*. 1994;65:79–83.
28. Giannobile WV, Finkelman RD, Lynch SE. Comparison of canine and non-human primate animal models for periodontal regenerative therapy: results following a single administration of PDGF/IGF-I. *J Periodontol*. 1994;65:1158–1168.